Reaction of Carbon Atoms, C ($2p^2$,^{3}P), with Hydrogen Sulfide, H_2S (X^1A_1): Overall Rate Constant and Product Channels

Nicolas Galland,[†] Françoise Caralp,[†] Marie-Thérèse Rayez,[†] Yacine Hannachi,*[,†,‡] Jean-Christophe Loison,[§] Gérard Dorthe,[§] and Astrid Bergeat*[,∥,§]

Theory Group and Experimental Group, Laboratoire de Physico-Chimie Moléculaire, CNRS UMR 5803, Université Bordeaux I, F-33405 Talence Cedex, France

Received: May 4, 2001; In Final Form: July 23, 2001

The multichannel C + H_2S reaction was studied, at room temperature, in a low-pressure fast-flow reactor. Carbon atoms were obtained from the reaction of CBr_4 with potassium atoms. The overall rate constant was found to be $(2.1 \pm 0.5) \times 10^{-10}$ cm^3 molecule^{-1} s^{-1}, close to the gas kinetic limit. Absolute product branching ratio was estimated over the channels yielding H atoms probed by resonance fluorescence in the vacuum ultraviolet: H + HCS or HSC (75 ± 25)%. Ab initio studies of the different stationary points relevant to this reaction have been performed at the CCSD(T)/cc-pVTZ//QCISD/cc-pVDZ level. In agreement with the measured rate constant, the insertion transition structure leading to triplet HSCH is found lower in energy than the reactants. The reaction is found to proceed via H_2SC ($^3A''$) intermediate that then rearrange to HSCH. On the basis of RRKM calculations, this last species leads mainly to HCS + H products.

I. Introduction

The C + H_2S reaction is believed to play a key role in combustion and interstellar chemistry, particularly in cold and dense clouds.[1] More specifically, sulfur compounds were observed in the collision of comet Shoemaker-Levy 9 with Jupiter, although sulfur species are not normally present in the Jovian atmosphere. On the other hand, ground-state atomic carbon, C($2p^2$ ^{3}P), has been detected in a wide range of astronomical environments and is particularly abundant in dense interstellar clouds.[2] It is thus interesting to study in detail the kinetics of the C + H_2S reaction. Despite its importance, there are, to our knowledge, only a few experiments or theoretical studies on the dynamics or the kinetics of this reaction.

The possible channels with the reaction enthalpies[3] at 298.15 K for the products in their ground electronic states are

$$C(^3P) + H_2S(X^1A_1) \rightarrow H_2(X^1\Sigma^+) + CS(X^1\Sigma^+) \qquad \Delta_r H^\circ_{298.15} = -99.4 \text{ kcal mol}^{-1}$$

$$\rightarrow H(^2S) + HCS(X^2A') \qquad \Delta_r H^\circ_{298.15} = -42.6 \text{ kcal mol}^{-1}$$

$$\rightarrow H(^2S) + HSC(X^2A')$$

$$\rightarrow S(^3P) + CH_2(X^3B_1) \qquad \Delta_r H^\circ_{298.15} = -7.8 \text{ kcal mol}^{-1}$$

$$\rightarrow 2\,H(^2S) + CS(X^1\Sigma^+, a^3\Pi) \qquad \Delta_r H^\circ_{298.15} = +4.8 \text{ kcal mol}^{-1}$$

$$\rightarrow CH(X^2\Pi) + HS(X^2\Pi) \qquad \Delta_r H^\circ_{298.15} = +8.9 \text{ kcal mol}^{-1}$$

The overall rate constant has been determined previously by G. Dorthe et al.[4] at room temperature in a fast-flow reactor, the carbon atoms being produced by microwave dissociation of CO. The rate constant was found to be $(8.3 \pm 1.8) \times 10^{-11}$ cm^3 molecule^{-1} s^{-1}. Atomic carbon decay was followed through CS($a^3\Pi$) chemiluminescence from C + OCS → CS($a^3\Pi$) + CO, observed when OCS was added to H_2S. However, they have never determined any product of the reaction.

Kaiser and co-workers[5] have carried out detailed dynamical studies, with crossed molecular beam scattering technique. Identification of the reaction products, made possible with their mass spectrometer, provides a major advantage over kinetic measurements based on monitoring the disappearance of atomic carbon. On the basis of the center of mass angular and translational energy flux distributions inferred from the experimental data, e.g., time-of-flight spectra and angular distributions, the reaction products, as well as involved collision complexes, are characterized. The studies performed at four different collision energies from 16.7 to 42.8 kJ mol^{-1} lead to the conclusion that mainly HCS is formed under single collision conditions as the cutoffs of the translational energy flux distribution agree with the reaction energy of the more stable isomer (HCS compared to HSC) and as the TOF spectra at m/e = 44 (CS) show the identical shapes as m/e = 45 (HCS), HCS^+ fragmenting partly to CS^+ in the electron impact ionizer. Further, no radiative association to any H_2CS isomer was observed at m/e = 46. They could not however exclude a small amount (less than 10%) of HSC or CS. Moreover, the experimental data were added ab initio calculations of the different singlet and triplet minima. Their conclusions were that the reaction is indirect and proceeds through a thiohydroxycarbene intermediate HCSH after the addition of the carbon atom to the sulfur atom

* Corresponding authors.
† Theory Group.
‡ Fax: (33) 557962521. E-mail: hannachi@cribx1.u-bordeaux.fr.
§ Experimental Group.
∥ Fax: (33) 557962521. E-mail: bergeat@cribx1.u-bordeaux.fr.

10.1021/jp011713m CCC: $20.00
Published on Web 10/10/2001

of H_2S and the formation of a triplet H_2SC intermediate, and that the incorporated carbon atom and the leaving H atom are located on opposite sites of the rotational axes. However, their studies do not distinguish between different possible exit transition states, in particular the possibility of an intersystem crossing between the singlet and the triplet surfaces, as well as the possible contribution of thioformaldehyde H_2CS at their lower collision energies, corresponding to a translational temperature of ≈1300 K.[5a]

To understand better the mechanism of the title reaction, we have performed new kinetics experiment using a clean source of carbon atoms (from the reaction of CBr_4 with potassium atoms). The experiments were performed at room temperature, in a low-pressure fast-flow reactor. The overall rate constant was found by following directly the decay of carbon atom resonance fluorescence signal, the diffusion corrections being validated in a previous study of carbon atom reactions.[6] The absolute product branching ratio was estimated over the channels yielding H atoms probed by resonance fluorescence in the vacuum ultraviolet. The electronically excited products could be detected over the range 110−900 nm. These experiments are coupled to new ab initio determination of various stationary points on the potential energy surface relevant to this reaction. The probability of intersystem crossing between the triplet and the singlet surfaces is estimated using the Landau−Zener expression. Then, RRKM kinetics calculations based on the ab intio data allow us to estimate the branching ratios between the different possible reaction paths.

II. Experimental Section

A. Ab Initio Calculations. The structure of stationary points along the $C(^3P) + H_2S$ reaction have been optimized using the quadratic configuration interaction method including single and double excitations, QCISD[7] with the correlation consistent polarized valence double-ζ (cc-pVDZ) basis set of Dunning and co-workers.[8] The harmonic vibrational frequencies have been computed at the same level of theory in order to characterize the stationary points as minima or saddle points, to obtain zero-point vibrational energy (ZPVE) and to generate force constant data needed in the intrinsic reaction coordinate (IRC) calculations. Total energies are refined at the CCSD(T) (coupled cluster with a single- and double-excitation and a perturbational estimate of triple excitations)/cc-pVTZ level[8,9] using QCISD/cc-pVDZ optimized geometries. ZPVE correction to energies is used without any scaling factor. Unless otherwise noted, the discussed energetics are those obtained at the CCSD(T)/cc-pVTZ//QCISD/cc-pVDZ with QCISD/cc-pVDZ ZPVE corrections. For the QCISD and CCSD(T) calculations the core electrons have been frozen. The minimum energy paths were traced at the QCISD level to confirm that the located transition structures connect the presumed minima. The intrinsic reaction coordinate (IRC) method[10] was computed in mass-weighted internal coordinates with a step size of 0.1 $amu^{1/2}$ bohr. All calculations have been carried out with the Gaussian 94 program.[11]

B. Experimental Section Fast-Flow Reactor with a Chemical Source of C Atoms. The fast-flow reactor has been described in detail elsewhere,[6] and only a brief description is thus given. It consists of a hollowed-out stainless steel block, in which a 36 mm inner diameter Teflon tube is inserted, with four perpendicular optical ports for chemiluminescence and laser-induced or atomic resonance fluorescence detections. The flow velocity in the reactor was 26.5 m s^{-1}, with He (>99.995%) as carrier gas, at a total pressure of 2.0 Torr. C atoms were obtained by the successive abstractions of halogen atoms of CBr_4 by atomic potassium vapor in a microfurnace ending into a nozzle. A glass tube introduced the halogenated compound between the furnace and the nozzle exit. The whole device, mixing C atoms escaping from the nozzle with H_2S, slid along the Teflon inner wall of the reactor. The distance between the window detection and the nozzle exit could vary over the range 0−100 mm with a 0.5 mm precision.

C atoms were produced in the reactant injector nozzle from the $CBr_4 + 4K \rightarrow C + 4KBr$ overall reaction, resulting from the successive abstractions of the Br atoms by the vaporized potassium. Whatever the microfurnace temperature, an excess of potassium atoms [K] > 20[CBr_4] was used. The limiting step in the C production should be either the second or the third Br abstraction.[6a] The results indicated that the production of C_2 by C + CBr is possible, and the relative importance of C_2 was thus estimated. In the conditions used for the C pseudo-first-order decay determination, C_2 was found at concentrations 2 orders of magnitude lower than those of C, so that C + CBr influence on C decay measurements could be neglected.[6a] In the conditions used for the determination of the $C + H_2S$ product branching ratios, we used low CBr_4 concentration with the maximum distance between the end of the glass tube and the nozzle aperture. Under these conditions, the C partial pressure was below 0.005 mTorr with a negligible amount of CBr and C_2 radicals. H_2S was used directly from the cylinder without further purification, and its purity was >97.5% (the main impurities were CS_2 and OCS below 2000 ppv). CBr_4 (99%) was also used without further purification.

Atoms were detected by their resonance fluorescence. Atom excitation was achieved with the microwave discharge lamp previously used to probe the atomic products of the CH + NO reaction.[6b] The flowing gas mixture previously used to obtain intense emission lines of N, H, and O atoms gave also C emission lines owing to CO and CO_2 impurities. A pure Helium flow (purity of 99.9999%) was preferred for the relative branching ratio determination on H production, as the flow of helium contains enough impurity to get intense and nonreverse H atomic resonance fluorescence. The general procedure for atomic detection has also been previously detailed.[6] We would only mention that the conditions of the presently reported experiments ensure the linear dependence of the atomic fluorescence vs both the lamp emission intensity and the C and H atom concentrations, for the two gases used for the lamp in this study. For $C(^3P)$, the transitions at 156.1 nm ($2s^12p^3\ ^3D^\circ \leftrightarrow 2s^22p^2\ ^3P$) and at 165.7 nm ($2s^23s^1\ ^3P^\circ \leftrightarrow 2s^22p^2\ ^3P$) were used, while for $H(^2S)$ the transition at 121.6 nm ($2p^1\ ^2P^\circ \leftrightarrow 1s^1\ ^2S$) was used.

III. Results

A. Potential Energy Surface. The optimized structures of the different minima and transition structures lying on the triplet surface are displayed in Figures 1 and 2, respectively, while the energy diagram along the reaction path is shown in Figure 3.

1. Relative Stability and Structures. The $C + H_2S$ triplet energy surface looks very similar to that of the valence isoelectronic $C + H_2O$ system.[12,13] There are three triplet multiplicity minima with CSH_2 stoichiometry: H_2SC **1** (C_s, $^3A''$), HSCH, **2** (C_1, ^3A), and H_2CS, **3** (C_s, $^3A''$). These species have been recently studied at a higher level of theory.[5a] The most stable species is H_2CS, with HSCH and H_2SC 22.3 and 76.3 kcal mol^{-1}, respectively, being higher in energy. The corresponding values obtained in the present study (22.2 and 76.4 kcal mol^{-1}) are virtually identical. The energy difference

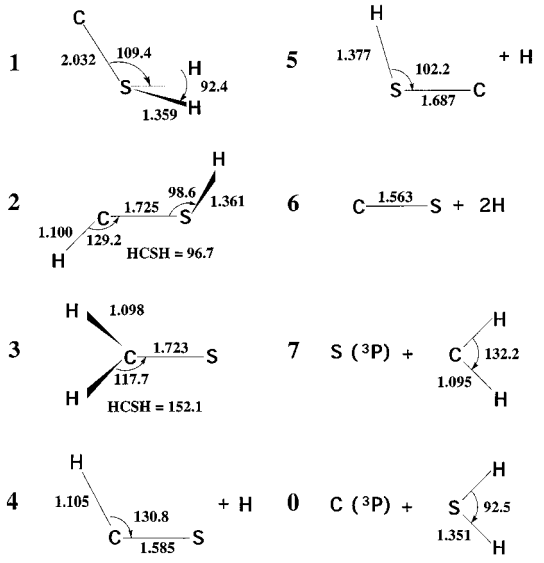

Figure 1. QCISD/cc-pVDZ optimized structures of minima. Distances in angstroms and angles in degrees. Dihedral angles (in degrees) are indicated ABCD = value. Value is the angle between ABC and BCD planes.

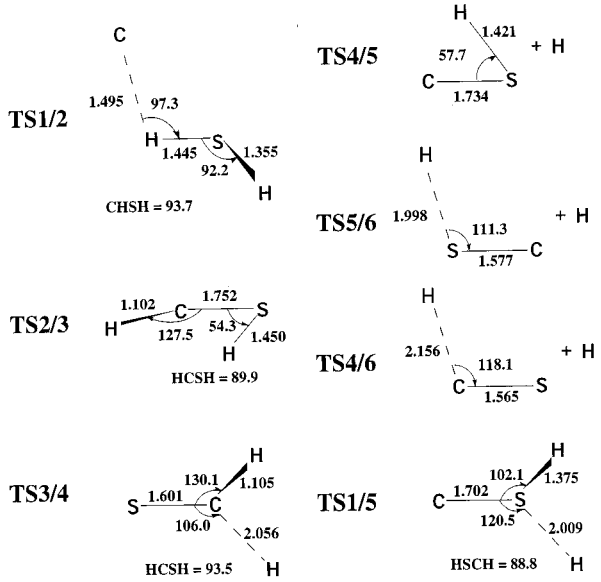

Figure 2. QCISD/cc-pVDZ optimized structures of transition structures. Same as those in Figure 1.

between triplet thioformaldehyde, H_2CS, and triplet thiohydroxycarbene, HCSH, was found in an early study[14] to be about 22.5 kcal mol^{-1}, very close to the present value. The C(^{3}P) + H_2S to H_2SC, HSCH, and H_2CS reaction energies obtained in this work (−13.8, −68.0, and −90.2 kcal mol^{-1}, respectively) are about 1.4 kcal mol^{-1} smaller than those obtained by Ochsenfeld et al.[5a] The agreement between the present values and those of a more elaborate level of theory is excellent.

The optimized structures (Figure 1) are very close to previous theoretical estimates. The H_2SC species has a carbon sulfur bond distance of 2.032 Å, longer than a typical CS single bond, and an out-of-plane angle between the C−S bond and the H_2S plane of 70.6°. This species is a charge-transfer complex. Mulliken charge on the carbon atom is −0.36 e at the QCISD/cc-pVDZ level. Hwang et al.[12] have also located this type of complex for the valence isoelectronic C−H_2O system. In this latter case, the binding energy (6.8 kcal mol^{-1}) is about half of that found for the H_2SC species. The CS bond length in the triplet thioformaldehyde H_2CS (1.723 Å) is overestimated by 0.04 Å (experimental[15] r_0(C−S) = 1.683 ± 0.005 Å). CCSD(T)/TZ2P value is slightly smaller (1.715 Å) but still larger that experimental r_0. The C−S bond length in triplet thiohydroxycarbene HCSH is almost identical to that of triplet thioformaldehyde H_2CS.

The energy difference between the HCS(^{2}A′) and HSC(^{2}A′) species is 38.5 kcal mol^{-1} in favor of the HCS isomer in agreement with the 39.6 kcal mol^{-1} obtained at CCSD(T)/QZ3P//CCSD(T)/QZ2P level of theory (with CCSD(T)/QZ2P ZPVE corrections) and other earlier theoretical predictions.[5a,14,16] The reactions leading to both species are exothermic. HSC species (+ H) is found, however, to be almost isothermic with the reactants (−1.8 kcal mol^{-1}), while HCS (+ H) is found 40.3 kcal mol^{-1} lower than the reactants. Somewhat larger values (−4.4 and −44.0 kcal mol^{-1}, respectively) were obtained at the CCSD(T)/QZ3P//CCSD(T)/QZ2P level of theory (with CCSD(T)/QZ2P ZPVE corrections). The optimized structures agree well with recent high level calculations.[5a,17,18]

2. Reaction Mechanism. Figure 3 displays a schematic picture of the potential energy surface (PES) correlating with carbon and hydrogen sulfide ground states. On the entrance channel, species **1** is formed without an energy barrier. The situation is similar to that of the C(^{3}P) + H_2O system. An insertion transition structure (**TS^1/$_2$**) is located connecting species **1** to triplet thiohydroxycarbene **2**. The energy barrier is about 8.1 kcal mol^{-1}. Of more importance, our calculations predict this transition structure 5.7 kcal mol^{-1} lower in energy than C(^{3}P) + H_2S. This contrasts with the C(^{3}P) + H_2O system,[12] where the insertion transition structure was found to be about 9 kcal mol^{-1} higher in energy than the reactants. Species **1** can also dissociate to HSC + H through **TS^1/$_5$** with a barrier of 15.7 kcal mol^{-1}. This transition structure is, however, 1.9 kcal mol^{-1} higher in energy than C(^{3}P) + H_2S. The barrier for hydrogen shift to form thioformaldehyde from thiohydroxycarbene (**TS^2/$_3$**) is 21 kcal mol^{-1}. The dissociation of thiohydroxycarbene HSCH to either HCS + H or HSC + H is found barrierless and endothermic by 27.7 and 66.2 kcal mol^{-1}, respectively. A barrier of 52.3 kcal mol^{-1} is found for the dissociation of thioformaldehyde H_2CS to HCS + H. The corresponding transition structure is only 2.4 kcal mol^{-1} higher than HCS + H. Species **3** can also dissociate to CH_2($^3B_1$) + S(^{3}P) without barrier. This reaction is endothermic by about 82 kcal mol^{-1}. Note that all stationary points on the channel leading to HCS + H and HSC + H (except **TS^1/$_5$**) are lower than the reactants. Attempt to localize a transition structure connecting H_2CS to H_2 + triplet CS was unsuccessful. The barrier for HCS to HSC isomerization is found about 57 kcal mol^{-1}, some 16 kcal mol^{-1} higher than C(^{3}P) + H_2S. HCS or HSC can further give CS($^1\Sigma$) + H but the corresponding transition structure are respectively 8.3 and 12.0 kcal mol^{-1} higher in energy than the initial reactants, C(^{3}P) + H_2S. In agreement with Pope et al.,[14] the dissociation of both HCS and HSC to CS + H is energetically more favorable than HCS/HSC isomerization.

On the light of this computed PES, the most energetically favorable channel (for low collision energy or low temperature) is the one leading to HCS + H with a much smaller probability for HSC + H or CH_2 + S. However, we have to point out that there are singlet H_2CS and HSCH (both cis and trans) lower in energy than the corresponding triplet species and intersystem crossing (ISC) is a possibility which might also lead to the formation of CS($X^1\Sigma^+$) diatomic (+ H_2) (see Figure 3). This

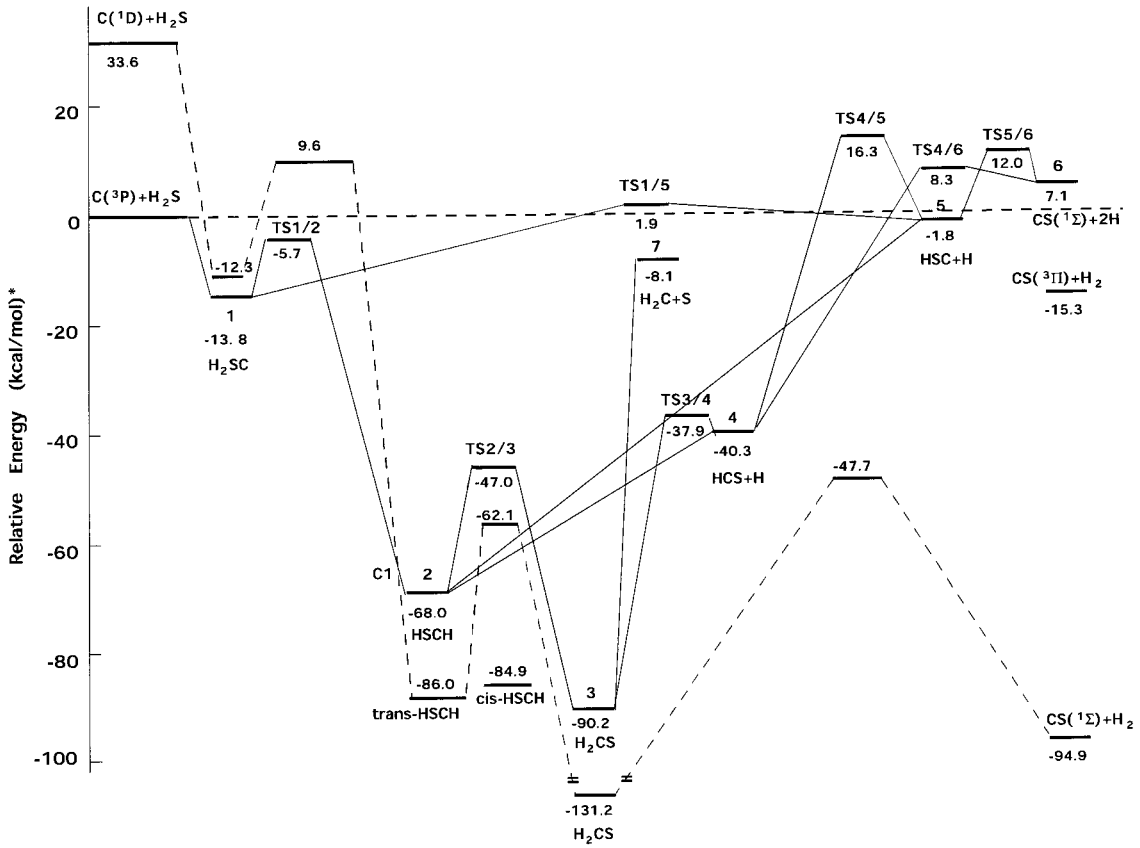

Figure 3. Schematic energy diagram along the reaction path: in solid lines, all the triplet paths involved in the reaction and in dotted lines, the most favorable singlet path leading to $CS(^1\Sigma^+) + H_2(^1\Sigma^+)$. Only the crossing point **C1** between the triplet HSCH and the singlet trans-HSCH is approximately shown. Energies, in kcal/mol, were computed using the CCSD(T)/cc-pVTZ//QCISD/cc-pVDZ method including QCISD/cc-pVDZ ZPVE.

issue will be discussed in the light of the experimental results and RRKM calculations combined with estimation of the ISC probability.

B. Experimental results. *1. Overall Rate Constant.* The pseudo-first-order decays of atomic carbon fluorescence were monitored at different concentrations of H_2S. Owing to the time needed to achieve the mixing of reactants, the decay became exponential at 2 cm from the nozzle through which escaped C atoms. The pseudo first-order rate constants were corrected from radial and axial diffusion from Keyser's formula:[19] $k_{cor} = k_{obs}[1 + ((a^2/48D) + D/v^2)k_{obs}]$, where k_{obs} is the observed first-order rate constant, a the radius of the reactor, v the average flow velocity, and D the diffusion coefficient of C atoms, equal to $860/P$ cm^2 s^{-1} where P is the total pressure in Torr.[4]

Values of the second-order rate coefficients were established by series of experiments in which the H_2S concentration and the total pressure (ranging from 1.1 to 2.6 Torr) were varied (Figure 4). The systematic deviation of the linear fit of the rate constant vs the H_2S concentration is close to 0.08×10^{-10}. However, the main source of errors in our measurements is the important radial and axial diffusions correction. Moreover, the high wall removal rate constant associated with these diffusions leads to the limit conditions of the plug−flow approximation. As a result, the error quoted was increased to contain all these uncertainties. An overall rate constant of $(2.1 \pm 0.5) \times 10^{-10}$ cm^3 molecule^{-1} s^{-1} was thus found for the C + H_2S reaction (Figure 4).

With the reactor used in the present study, but with carbon atoms being produced by the microwave dissociation of CO, Dorthe et al.[4] had previously found for this reaction a value of $(8.3 \pm 1.8) \times 10^{-11}$ cm^3 molecule^{-1} s^{-1}. Atomic carbon decay

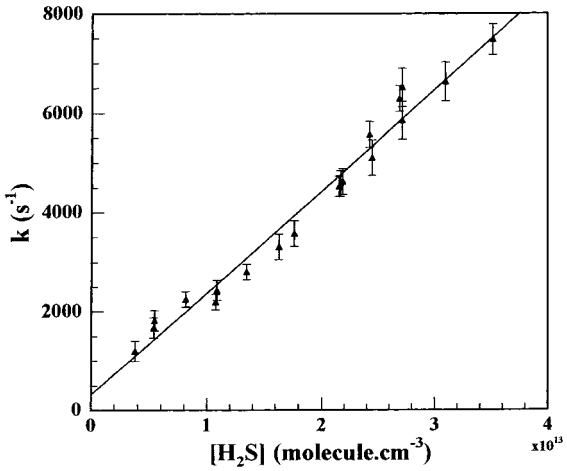

Figure 4. Plot of the pseudo-first-order rate constant of the C + H_2S reaction vs the H_2S concentration. The gradient of the fitted line yields the second-order rate constant, $k = (2.1 \pm 0.5) \times 10^{-10}$ cm^3 molecule^{-1} s^{-1}.

was followed through $CS(a^3\Pi)$ chemiluminescence from C + OCS → $CS(a^3\Pi)$ + CO, observed when OCS was added to H_2S. The discrepancy between the two sets of experiments is ascribed to the fact that $CS(a^3\Pi)$, being a long-lived species,[20] has a chemiluminescence decay which is slower than that of atomic carbon. The discrepancy was the same for the studies of the C + NO and C + O_2 reactions. However, our new determinations[6a] on C + O_2 and C + NO reactions were consistent with the values reported by Husain and Young,[21] which allow us to be more confident with the new determination of the C + H_2S reaction rate constant.

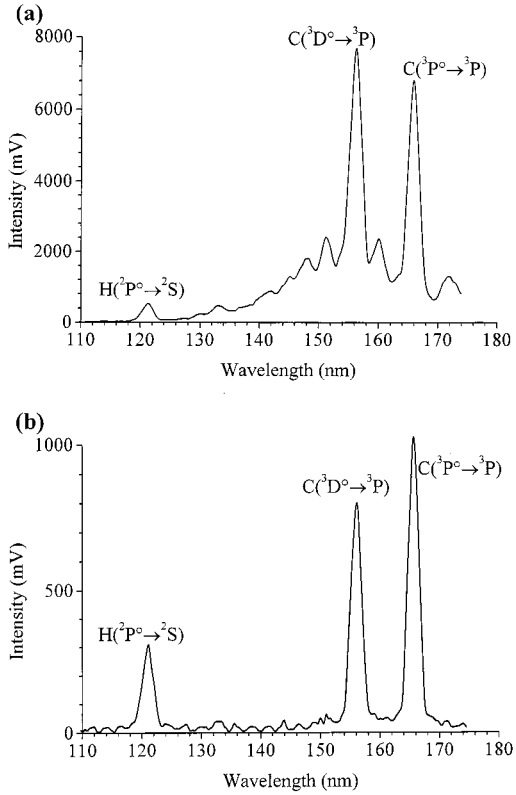

Figure 5. (a) Typical atomic emission spectrum of the microwave discharge lamp. (b) Typical atomic resonance fluorescence during the C + H_2S reaction study.

2. Product Branching Ratios. The CS($a^3\Pi$) chemiluminescence was detected around 360 nm. According to the decay of the chemiluminescence vs the distance, the excited CS seemed to be a primary product. However, the H_2S cylinder contains impurities, which could explain this chemiluminescence. A comparison with the signal obtained by the reaction of carbon atoms with OCS was performed. For this purpose, the H_2S gas was replaced by OCS gas, the carbon atom density being constant. The chemiluminescence intensity produced by the C + H_2S reaction represented 0.6% of the signal produced by the C + OCS reaction, with the atomic carbon densities and the observed first-order rate constants being the same. Because the impurities in the H_2S cylinder are 2000 ppm of OCS and 2000 ppm of CS_2, the chemiluminescence signal could thus be due to these impurities.

For the C + H_2S reaction, the H(^{2}S) atomic product was also probed. It is difficult to determine the absolute branching ratio for the production of hydrogen atoms by the C + H_2S reaction. Therefore, only an estimation could thus be done. The relative carbon and hydrogen atoms densities were determined by resonance fluorescence in the vacuum ultraviolet. First, it was checked that the atomic absorption was small. In this condition, the fluorescence signal divided by the emission intensity is proportional to $f_A[A]/\delta_A$, [A] being the atomic concentration, f_A the oscillator strength,[22] and δ_A the Doppler broadening (T = 300 K).[23] A typical atomic fluorescence spectrum is shown in Figure 5. It was obtained during the beginning of the C + H_2S reaction.

An example of the traces of C and H atoms concentrations, deduced from the fluorescence intensities, vs the distance, i.e., the reaction time, is shown in Figure 6. The C intensity decays, even if no H_2S is added. In its early stages, the decay of the observed C signal resulted mainly from the lowering of C density by the diffusion needed to fill a cross section of the

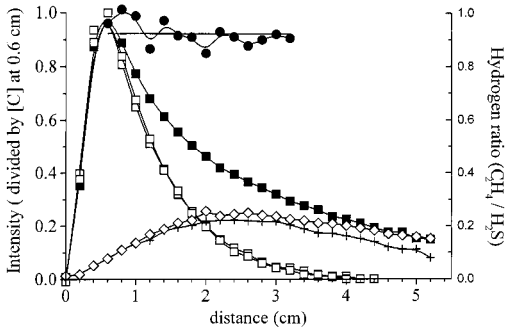

Figure 6. Relative traces of C(^{3}P), H(^{2}S) densities for the C + H_2S and C + C_2H_4 reactions. ■: carbon alone. □: carbon with H_2S or C_2H_4. ◇: hydrogen from the C + H_2S reaction. +: hydrogen from the C + C_2H_4 reaction. ●: ratio of H density from C + C_2H_4 divided by H density from C + H_2S.

reactor (36 mm) after the nozzle exit (14 mm). Then, the decay of the observed C signal was due to the wall removal reaction or to the reaction with H_2S, when added. Because the H_2S gas had also to diffuse to fill a cross section of the reactor, the C + H_2S reaction itself was delayed by mixing effects. This effect was reduced by a device mixing C atoms escaping from the nozzle, with H_2S used for the studies of the overall rate constant. However, to determine the relative ratio of H production on C consumption, it was preferred to perform the studies without the mixing device, to limit the perturbations due to the wall removal reactions. In fact, the wall removals became thus important only at the last stages of the C traces and of the H traces. Because the carbon production is constant within a period of more than 1 h, the carbon concentration without and with H_2S, and then the hydrogen concentration were measured successively vs the distance. This operation was repeated alternately for different H_2S concentrations and under different pressures, several times. That way, the major incertitude is secondary reactions. It was thus checked that secondary products of our chemical source did not interfere in the results. The possible secondary products are CBr and C_2 radicals (C_2 being produced by the C + CBr reaction) and also K and KBr. K and KBr cannot produce H atoms with H_2S. CBr and C_2 concentrations are lower by at least a factor of 10 and 20, respectively.[6a] Thus, these radicals could only play a minor role in our experimental conditions. It was confirmed by the experiments on the C + hydrocarbon reactions.[24] Actually, the ratio of hydrogen production from C + H_2S to the one from the C + hydrocarbon reaction was constant, even at long distance.

We thus tried to measure the absolute branching ratio, by simulating all the parameters of the reactions, particularly the wall removal reactions and the expansion term (for the measurement of the hydrogen production, the convector was not used). The various fitting parameters lead to an important uncertainty. An absolute hydrogen production was estimated to be between 50 and 100% for the C + H_2S reaction. Moreover, the hydrogen production of the C + H_2S reaction was compared with those obtained by the C + acetylene, ethylene, or benzene reactions.[24] The C + H_2S reaction leads to the highest hydrogen production. The relative atomic hydrogen production from the C + C_2H_4 reaction compared to the H production from the C + H_2S reaction is 0.92 ± 0.04. Now, the last ab initio calculations performed by Le et al.[25] on the C + ethylene reaction lead to the conclusion that the H product branching ratio is 98%.

IV. Discussion

Five different product channels are exothermic for the C + H_2S reaction. The present calculated reaction energies are

$$C(^3P) + H_2S(X^1A_1)$$

$$\rightarrow H_2(X^1\Sigma^+) + CS(X^1\Sigma^+) \qquad -94.9 \text{ kcal mol}^{-1}$$

$$\rightarrow H_2(X^1\Sigma^+) + CS(a^3\Pi) \qquad -15.3 \text{ kcal mol}^{-1}$$

$$\rightarrow H(^2S) + HCS(X^2A') \qquad -40.3 \text{ kcal mol}^{-1}$$

$$\rightarrow H(^2S) + HSC(X^2A') \qquad -1.8 \text{ kcal mol}^{-1}$$

$$\rightarrow CH_2(X^3B_1) + S(^3P) \qquad -8.1 \text{ kcal mol}^{-1}$$

In view of the schematic energy diagram along the reaction path shown on Figure 3, we need to address four preliminary points. First, the saddle point **TS^1/$_5$**, being located at 1.9 kcal mol^{-1} above the energy level of the reactants and 7.6 kcal mol^{-1} above the saddle point **TS^1/$_2$**, the $^1/_5$ channel leading to H + HSC, must be negligible at 298 K. However, if an uncertainty on the determination of energy barriers is taken into account, the possible occurrence of this way cannot be a priori discarded and must be evaluated. Second, as the HCS and HSC species have been observed in the interstellar medium, it is thus interesting to evaluate the branching ratios for the C + H_2S reaction. Moreover, the CH_2 + S channel could be a competitive channel for the H + HSC channel. Third, the most exothermic channel yielding to $H_2(X^1\Sigma^+)$ + $CS(X^1\Sigma^+)$ is spin forbidden and has to go through intersystem triplet−singlet crossing. We have to evaluate the possiblity of the occurrence of this intersystem crossing. Fourth, the attempt to localize a transition structure, lower in energy than the reactants or with a small barrier, by connecting H_2CS to $H_2(X^1\Sigma^+)$ + $CS(a^3\Pi)$ was unsuccessful, as explained in the theoretical previous section. The channel, leading to $H_2(X^1\Sigma^+)$ + $CS(a^3\Pi)$, is thus impossible under the interstellar conditions or at room temperature, which is in agreement with our experimental study, confirming that no or a very small amount of $CS(a^3\Pi)$ is produced by the reaction. Answers to the first three questions can be derived from microcanonical statistical RRKM calculations and confirmed by the following experimental results.

According to the studies performed by the crossed molecular beam technique by Kaiser and co-workers,[5] mainly HCS is formed under single collision conditions and the reaction is indirect and proceeds through the thiohydroxycarbene intermediate HCSH (species **2**). However, as they themselves recognize, their studies are unable to eliminate the possibility of an intersystem crossing or the contribution of the thioformaldehyde intermediate H_2CS (species **3**). Moreover, the collision energies of the reactants C + H_2S in their experiments were higher than 4 kcal mol^{-1}, which could imply the channel via transition structure **TS^1/$_5$**, lying about 1.9 kcal mol^{-1} higher in energy than the reactants. At room temperature or lower temperature, as in the interstellar medium, this channel must be negligible. Our experimental study confirms that no or a very small amount of $CS(a^3\Pi)$ is produced by the reaction. However, the two experimental studies are unable to determine the ratio HCS/HSC produced by the reaction and the possibility of an intersystem crossing. Then microcanonical statistical RRKM calculations have been performed.

The microcanonical rate constants of the various steps of the mechanism are obtained from the classical RRKM expression.

$$k(E) = \frac{G(E)}{hN(E)}$$

In this expression h is the Planck's constant, $G(E)$ is the number of energetically accessible states at the transition state, and $N(E)$ is the density of states of the intermediate species. All species are treated as symmetric tops and the external K-rotor, associated with the smallest moment of inertia is treated as an active degree of freedom completely coupled with vibrations. For the steps that proceed through saddle point, the density of states for the reacting molecule and the sum of states for the transition state are derived by taking the inverse Laplace transform of the corresponding partition functions calculated with the structural parameters obtained from ab initio calculations. For the exit channels $^2/_4$, $^2/_5$, or $^2/_7$, where no barrier is involved in the inverse association reaction, the microvariational theory MVIPF[26] (microcanonical variational theory by inversion of the interpolated partition function) is implemented to determine the loose transition state variationally along the reaction coordinate. In this procedure, the interpolation parameter of a switching function between the partition functions of reactants and products is adjusted in such a manner that the calculated thermal dissociation rate constant multiplied by the equilibrium constant yields the experimental value of the thermal association rate constant at the high-pressure limit.

TABLE 1: Intermediate Species Lifetimes at E = 1 kcal mol^{-1} [a]

	species		
	1	**2**	**3**
τ (ps)	0.62	0.064	0.056

[a] Origin of the energy at the energy level of the reactants.

The lifetime τ of the various species for an energy E is then obtained from $1/\tau = \sum_i k_i(E)$, where $k_i(E)$ are the microcanonical constants of all steps in the mechanism in which the corresponding species is implicated.

The initial energy distribution function of the energized H_2SC^* radical (species **1**) is determined by detailed balance assuming thermal energy distribution on the reactants H_2S + C.[29] At 298 K, the maximum of this distribution is located at ca. 0.6 kcal mol^{-1} (230 cm^{-1}) above the energy level of the reactants and its half-height width is about 1.7 kcal mol^{-1} (600 cm^{-1}). Taking into account the narrowness of this distribution and the large excess energy of the adduct H_2SC^* above the energy level of the species **2** and **3**, it will be assumed that H_2SC^* is monoenergetically energized with an energy of 1 kcal mol^{-1} (350 cm^{-1}) above the energy level of the reactants.

The lifetimes of the various species are determined from the two previous expressions. For calculating the microcanonical rate constant of the barrierless steps $^2/_4$, $^2/_5$, and $^2/_7$, the variational procedure is used as described above, assuming that $k_{(H + HCS)}$, $k_{(H + HSC)}$, and $k_{(S + HCH)} = 1 \times 10^{-10}$ cm^3 molecule^{-1} s^{-1} at the high-pressure limit, based on the rate constants of the H + HCO[27] and O + HCH[28] reactions. The calculated microcanonical constants of different steps in the mechanism and unimolecular lifetimes of the intermediate species are presented in Tables 1 and 2. The H_2SC^* RRKM lifetime (0.6×10^{-12} s) meets the ergodicity criterion and is short enough to be able to neglect collisional energy loss (the collision frequency for 1 atm. of air at 298 K is $\approx 10^{10}$ s^{-1}). Indeed, chemical activation experiments have enabled the rate constants for randomization to be determined and led to values of the order of 10^{12} s^{-1}.[29] Thus, these calculations show just that the lifetimes of the transitions species **2** and **3** are very short.

The negligible contribution of the **TS^{1}5** pathway can be derived from the previous microcanonical statistical RRKM calculations. The calculated rate constants of the step $^1/_2$ and $^1/_5$ are $k_{1/2}(E) = 1.6 \times 10^{12}$ s^{-1} and $k_{1/5}(E) = 0$. If we assume

TABLE 2: Microcanonical Constants of Different Steps in the Reaction Mechanism at Different Energy *E* above the Energy of the Reactants in Their Ground State

steps	$^1/_2$	$^1/_5$	$^2/_1$	$^2/_3$	$^3/_2$	$^2/_4$	$^3/_4$	$^2/_5$	$^3/_7$
k (s^{-1}) for $E = 1$ kcal mol^{-1}	1.6×10^{12}	0	6.5×10^{9}	3.5×10^{12}	3.3×10^{12}	1.2×10^{13}	1.4×10^{13}	7.2×10^{9}	5.5×10^{11}
k (s^{-1}) for $E = 5$ kcal mol^{-1}	2.8×10^{12}	2.8×10^{11}	9.9×10^{9}	3.9×10^{12}	3.9×10^{12}	1.3×10^{13}	2.0×10^{13}	3.7×10^{10}	6.4×10^{11}
k (s^{-1}) for $E = 10$ kcal mol^{-1}	4.4×10^{12}	2.3×10^{12}	3.2×10^{10}	4.3×10^{12}	4.6×10^{12}	1.5×10^{13}	2.6×10^{13}	1.3×10^{11}	1.4×10^{12}

a decrease of 2 kcal mol^{-1} on the value of energy level of **TS^1/$_5$**, due to the uncertainty of the ab initio calculations, $k_{1/5}(E) = 6 \times 10^{10}$ s^{-1} results. This last value is 20 times lower than $k_{1/2}$. This calculation allows us to state that the production of the HSC radical via the transition structure **TS^1/$_5$** is negligible at room temperature and a fortiori at the lowest interstellar temperatures where the energy distribution will be narrower. Under the conditions of the experimental studies of Kaiser and co-workers[5] on the dynamics of the C + H_2S, the reaction was found to be indirect and to proceed through the thiohydroxycarbene intermediate HCSH (species **2**), but their collision energies were higher than 4 kcal mol^{-1}. The RRKM calculations confirm that this pathway is negligible at the lowest interstellar temperatures, but becomes competitive at higher energy (see Table 2).

The second point to be discussed was the relative branching ratio between the channels leading to H + HCS, H + HSC and CH_2 + S. Kaiser's experiment and our experiment agree that the main channel leads to the formation of atomic hydrogen. However, none of us were able to determine the relative branching ratio HCS/HSC. RRKM calculations on Table 2, show that the microcanonical rate constant of channel HCSH (**2**) → H + HCS (**4**) is 1667 times higher than one of channel HCSH (**2**) → H + HSC (**5**). Moreover, it is possible to produce HCS via H_2CS (**3**) which could also lead to CH_2 + S (**7**). However, on the basis of calculated microcanonical rate constants, 25 time less CH_2 + S would be formed than HCS + H via species **3**. In conclusion, the main reaction channel is the one leading to H + HCS via species **2**, the thiohydroxycarbene HCSH. More specifically, the RRKM calculations give the following branching ratios: H + HCS, 99.22% (80.75% via species **2** and 18.47% via species **3**); H + HSC, 0.05%; and S + CH_2, 0.73%.

However, the most exothermic channel leads to $H_2(X^1\Sigma^+)$ + $CS(X^1\Sigma^+)$, but is spin forbidden and has to go through intersystem triplet−singlet crossing (see Figure 3). This intersystem crossing is possible as there are singlet species lower in energy than the corresponding triplet species **2** and **3**; the singlet HCSH intermediate species **2** lies 86 kcal mol^{-1} lower than the reactants energy, and the singlet H_2CS intermediate species **3**, 131.2 kcal mol^{-1} lower. On the other hand, the singlet CSH_2 intermediate species **1** and transition structure **TS^1/$_2$** were found to have energies of −12.3 and +9.6 kcal mol^{-1}, respectively. Moreover, the singlet CSH_2 intermediate species **1** and transition structure **TS^1/$_2$**, with the optimized structures of the triplet ones, lie about 25.5 and 24.1 kcal mol^{-1}, respectively, higher in energy than the triplet states. Thus, the intersystem crossing possibilities occur between the transition structure **TS^1/$_2$** and the HCSH intermediate species **2**.

The probability of a curve crossing can be estimated by the Landau−Zener expression:

$$P_{T\rightarrow S} = 1 - \exp\left[\frac{2\pi\Delta E_x^2}{\hbar v|\Delta F_x|}\right]$$

where ΔE_x is the finite gap between the two potential curves at the crossing point, $|\Delta F_x|$ is the absolute value of the difference in slopes at the crossing point, and v the nucleus velocity at the crossing point. To estimate the slopes of the singlet and triplet surface and the spin−orbit coupling, we have located the approximate singlet triplet intersection for the HCSH isomer. We used state average CASSCF calculations with Slater determinant to optimize a "conical intersection"[30,31] within a two-electron, four-orbital active space (CAS(2,4)) and the cc-pVTZ basis set. The geometrical parameters of the crossing points between the triplet HSCH and the singlet trans-HSCH (**C1**) and the singlet cis-HSCH (**C2**) are depicted in Figure 7. A single-point calculation at the CCSD(T)/cc-pVTZ level shows that the activation energy for the rearrangement of triplet HSCH to singlet trans-HSCH is less than 2 kcal mol^{-1} (3.7 kcal mol^{-1} for the rearrangement to singlet cis-HSCH). The calculated spin−orbit coupling[32] between the singlet and triplet electronic states is 29 and 23 cm^{-1} for **C1** and **C2**, respectively. Since, in this part of the hypersurface, the main reaction coordinate is the HSCH dihedral angle, we estimate the slope of the surfaces using a two points finite difference calculations at the CCSD-(T)/cc-pVTZ by varying the HSCH dihedral angle from its value at the crossing point toward the corresponding minimum. The differences in slopes $|F_x|$ are thus 0.03 hartree $bohr^{-1}$ rad^{-1} for trans-HSCH intersystem crossing point, and 0.02 hartree $bohr^{-1}$ rad^{-1} for cis-HSCH intersystem crossing point. The calculations based on the geometrical changes in distance between the C atom and H_2S lead to the same result. We could then conclude that in the intersystem crossing region (on the real 6-fold surface), the difference in slopes $|F_x|$ is ≈ 0.03 hartree $bohr^{-1}$ rad^{-1}. Then, the velocity of the nuclei at the intersection point can be estimated by the expression:

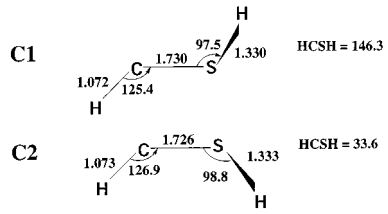

Figure 7. CAS(2,4)/cc-pVTZ T_1-S_0 conical intersection leading to singlet trans-HSCH (**C1**) and cis-HSCH (**C2**).

$$v = r\omega = \sqrt{2E/\mu_{H-CSH}}$$

where E is the translational energy of the nuclei and μ the reduced mass of the system H-CSH. The value of E depends on the exact localization of the crossing point. The intersystem crossing calculated for HCSH (species **2**) gives a value of E around 67.0 kcal mol^{-1}, but on all the internal degrees of freedom. Because all the internal modes could participate to the crossing, we could consider that the velocity of the nuclei should be close to 1.1×10^{-2} $hartree^{1/2}$ $emu^{-1/2}$ (1822.888 electron mass unit = 1 proton mass ≈ 1 atomic mass unit). The last parameter is ΔE_x, which is generally much smaller than the asymptotic (or nominal) value of ΔE, the spin−orbit coupling. In a first approximation, we will consider the most favorable case for the ISC, $\Delta E_x \approx 29$ cm^{-1}, i.e., 1.32×10^{-4} hartree, calculated for **C1**.

The probability that there is a change in electronic state during the passage of the system through the critical region is thus, in

the most favorable case, around 0.03%. However, this value is the probability of ICS for each intersystem crossing point on the reactive surface. We have then to evaluate if the lifetimes of the different transition species allow an intersystem crossing to happen, by increasing the number of passages through the critical region. RRKM calculations can answer to this question: the calculated unimolecular lifetimes of the intermediate species are very short, around 0.06 ps, which is on the order of a vibrational period. Because we could thus expect only one passage through the intersystem crossing point, the intersystem crossing is not favored by this very small lifetime of the intermediates. In conclusion, the probability of triplet−singlet crossing is thus negligible and only the H + HCS products are formed.

V. Conclusion

The atomic carbon adds to hydrogen sulfide to form a CSH_2 complex intermediate. This first reaction step does not present any activation energy and is exothermic by 13.8 kcal mol^{-1}. This triplet intermediate rearranges to the triplet thiohydroxycarbene, HCSH. Even if the singulet state of this intermediate is lower in energy, the transfer probability to the singlet potential energy surface through intersystem crossing is very small, and thus the $CS(X^1\Sigma^+) + H_2(X^1\Sigma^+)$ products corresponding to the most exothermic channel are not formed. The triplet intermediate HCSH can easily decompose to H + HCS without exit barrier. The channel leading to H + HSC is only ≈1.8 kcal mol^{-1} exothermic with respect to the reactants, and is thus negligible compared to the one leading to H + HCS ≈ 40.3 kcal mol^{-1}. Moreover, the HCSH intermediate possesses enough energy to rearrange to thioformaldehyde isomer H_2CS, which can lead to the H + HCS via a transition structure with a small barrier, or to CH_2 + S without any barrier. The HCS isomerization to HSC is unable at room or lower temperature as the transition structure presents a barrier 16.3 kcal mol^{-1} higher than the reactant energy. No pathway yielding to $CS(a^3\Pi) + H_2(X^1\Sigma^+)$ was found open for small total available energy of the reactants. All these theoretical results are in agreement with the experimental data. The overall rate constant was found to be close to the gas kinetics limit: $k_{C+H_2S} = (2.1 \pm 0.5) \times 10^{-10}$ cm^3 $molecule^{-1}$ s^{-1}. Our experimental study on chemiluminescence detection confirms that no or a very small amount of $CS(a^3\Pi)$ is produced by the reaction. With the kinetics studies on H and C resonance fluorescence signals, absolute H production was estimated to be between 50 and 100%. However, the relative H production from the C + C_2H_4 reaction compared to the H production from the C + H_2S reaction was found to be 0.92 ± 0.04. Because the RRKM calculations[25] performed on the C + C_2H_4 reaction lead to a H branching ratio of 98%, we could conclude that the H atom is nearly the exclusive product of the C + H_2S reaction. Our RRKM calculations confirm that the product branching ratio over the channels yielding H atoms is close to the unity for the C + H_2S reaction, and more exactly corresponding to the HCS product.

Acknowledgment. Y.H. thank the "Institut du Developpement et des Ressources en Informatique Scientifique" (CNRS, IDRIS) for providing computer facilities (Project 0337).

References and Notes

(1) Milar, T. J.; Herbst, E. *Astron. Astrophys.* **1990**, *231*, 466.

(2) Henning, Th.; Salama, F. *Science* **1998**, *282*, 2204.

(3) Mallard, W. G., Linstrom, P. J., Eds. *NIST Chemistry WebBook, NIST Standard Reference Database Number 69*; National Institute of Standards and Technology: Gaithersburg MD, 20899, February 2000 (http://webbook.nist.gov).

(4) Dorthe, G.; Caubet, P.; Vias, T.; Barrère, B.; Marchais, J. *J. Phys. Chem.* **1991**, *95*, 5109.

(5) (a) Ochsenfeld, C.; Kaiser, R. I.; Lee, Y. T.; Head-Gordon, M. *J. Chem. Phys.* **1999**, *110*, 9982. (b) Kaiser, R. I.; Ochsenfeld, C.; Head-Gordon, M.; Lee, Y. T. *J. Chem. Phys.* **1999**, *110*, 2391. (c) Kaiser, R. I.; Ochsenfeld, C.; Stranges, D.; Head-Gordon, M.; Lee, Y. T. *Faraday Discuss.* **1998**, *109*, 183. (d) Kaiser, R. I.; Ochsenfeld, C.; Head-Gordon, M.; Lee, Y. T. *Science* **1998**, *279*, 1181. (e) Kaiser, R. I.; Sun, W.; Suits, A. G. *J. Chem. Phys.* **1997**, *106*, 5288.

(6) (a) Bergeat, A.; Calvo, T.; Dorthe, G.; Loison, J.-C. *Chem. Phys. Lett.* **1999**, *308*, 7. (b) Bergeat, A.; Calvo, T.; Daugey, N.; Loison, J.-C.; Dorthe, G. *J. Phys. Chem. A* **1998**, *102*, 8124.

(7) Pople, J. A.; Head-Gordon, M.; Raghavachari, K. *J. Chem. Phys.* **1987**, *87*, 5968.

(8) Dunning, T. H., Jr. *J. Chem. Phys.* **1989**, *90*, 1007.

(9) Raghavachari, K.; Trucks, G. W.; Pople, J. A.; Head-Gordon, M. *Chem. Phys. Lett.* **1989**, *157*, 479.

(10) (a) Fukui, K. *J. Chem. Phys.* **1977**, *66*, 2153. (b) Gonzalez, C.; Schlegel, H. B. *J. Phys. Chem.* **1990**, *94*, 5523.

(11) Frisch, M. J.; Trucks, G. W.; Schlegel, H. B.; Gill, P. M. W.; Johnson, B. G.; Robb, M. A.; Cheeseman, J. R.; Keith, T.; Petersson, G. A.; Montgomery, J. A.; Raghavachari, K.; Al-Laham, M. A.; Zakrzewski, V. G.; Ortiz, J. V.; Foresman, J. B.; Cioslowski, J.; Stefanov, B. B.; Nanayakkara, A.; Challacombe, M.; Peng, C. Y.; Ayala, P. Y.; Chen, W.; Wong, M. W.; Andres, J. L.; Replogle, E. S.; Gomperts, R.; Martin, R. L.; Fox, D. J.; Binkley, J. S.; Defrees, D. J.; Baker, J.; Stewart, J. P.; Head-Gordon, M.; Gonzalez, C.; Pople, J. A. *Gaussian 94*, revision D. 4; Gaussian, Inc.: Pittsburgh, PA, 1995.

(12) Hwang, D.-Y.; Mebel, A. M.; Wang, B.-C. *Chem. Phys.* **1999**, *244*, 143.

(13) Yamaguchi, Y.; Wesolowski, S. S.; Van Huis, T. J.; Schaefer, H. F., III. *J. Chem. Phys.* **1998**, *108*, 5281.

(14) Pope, S. A.; Hillier, I. H.; Guest, M. F. *J. Am. Chem. Soc.* **1985**, *107*, 3789.

(15) Judge, R. H.; Moule, D. C.; King, G. W. *J. Mol. Spectrosc.* **1980**, *81*, 37.

(16) Curtiss, L. A.; Nobes, R. H.; Pople, J. A.; Radom, L. *J. Chem. Phys.* **1992**, *97*, 6766. (b) Bunker, R. J.; Bruna, P. J.; Peyerimhoff, S. D. *Isr. J. Chem.* **1984**, *19*, 309. (c) Stoecklin, T.; Halvick, Ph.; Rayez, J.-C. *J. Mol. Struct., Theochem.* **1988**, *163*, 265. (d) Stoecklin, T. Thèse de L′Université Bordeaux I, Bordeaux, France, 1989.

(17) Petraco, N. D. K.; Wesolowski, S. S.; Leininger, M. L.; Schaefer, H. F., III. *J. Chem. Phys.* **1998**, *108*, 5281.

(18) Senekowitsch, J.; Carter, S.; Rosmus, P.; Werner, H.-J. *Chem. Phys.* **1991**, *147*, 281.

(19) Keyser, L. F. *J. Phys. Chem.* **1984**, *88*, 4750.

(20) Moltzen, E. K.; Klabunde, K. *J. Chem. Rev.* **1988**, *88*, 393.

(21) Husain, D.; Young, A. N. *J. Chem. Soc., Faraday Trans. 2* **1975**, *71*, 525.

(22) Wiese, W.; Fuhr, J.; Deters, T. *J. Phys. Chem. Ref. Data, Monogr.* **1996**, *7*.

(23) Lynch, K. P.; Schwab, T. C.; Michael, J. V. *Int. J. Chem. Kinet.* **1976**, *8*, 651.

(24) Bergeat, A.; Loison, J.-C. *PCCP* **2001**, *3*, 2038.

(25) Le, T. N.; Lee, H.; Mebel, A. M.; Kaiser, R. I. *J. Phys. Chem. A* **2001**, *105*, 1847.

(26) Forst, W. *J. Phys. Chem.* **1991**, *95*, 3612.

(27) Timonen, R. S.; Ratajczak, E.; Gutman, D. *J. Phys. Chem.* **1987**, *91*, 692.

(28) Baulch, D. L.; Cobox, C. J.; Cox, R. A.; Esser, C.; Frank, P.; Just, Th.; Kerr, J. A.; Pilling, M. J.; Troe, J.; Walker, R. W.; Warnatz, J. *J. Phys. Chem. Ref. Data* **1992**, *21*, 411.

(29) Ho*l*brook, K. A.; Pilling, M. J.; Roberston, S. H. *Unimolecular Reaction*, 2nd Ed.; John Wiley & Sons Ltd.: Chichester, 1996.

(30) Bearpark, M. J.; Robb, M. A.; Schlegel, H. B. *Chem. Phys. Lett.* **1994**, *223*, 269.

(31) Ragazos, I. N.; Robb, M. A.; Bernardi, M.; Olivucci, M. *Chem. Phys. Lett.* **1992**, *197*, 217.

(32) Abegg, P. W. *Mol. Phys.* **1975**, *30*, 579.